Observation of CN $A \rightarrow X$ and $B \rightarrow X$ emissions in gas-phase collisions of fast $O(^3P)$ atoms with HCN

O. J. Orient, A. Chutjian, and K. E. Martus
Jet Propulsion Laboratory, California Institute of Technology, Pasadena, California 91109

E. Murad
Phillips Laboratory/WSSI, Hanscom Air Force Base, Bedford, Massachusetts 01731

(Received 18 January 1993)

Optical emissions in single-collision reactions of fast (5–25-eV translational energy) $O(^3P)$ atoms with HCN have been measured in a crossed-beam geometry. The emissions were observed in the wavelength range 345–430 and 550–825 nm, and were identified as the CN($B\,^2\Sigma^+ \rightarrow X\,^2\Sigma^+$) and CN($A\,^2\Pi_i \rightarrow X\,^2\Sigma^+$) transitions, respectively. The experimental $B \rightarrow X$ vibrational bands were found to fit a synthetic spectrum of CN at a vibrational temperature of 7000 K (0.60 eV) and a rotational temperature of 2000 K (0.17 eV). The $A \rightarrow X$ spectra were simulated in terms of known Franck-Condon factors for that band system. The energy threshold for the CN($B \rightarrow X$) emission was measured to be 7.4±0.8 eV (lab) or 4.6±0.5 eV (c.m.), which agrees with the energy threshold for the reaction $O(^3P)+HCN(\tilde{X}) \rightarrow OH(X)+CN(B)$.

PACS number(s): 34.50.Lf

I. INTRODUCTION

Detailed studies of the reaction of fast neutral atoms with molecular targets under single-collision (nonplasma) conditions enables one to follow the transition between endoergic and exoergic reactions. Reaction channels which are normally closed under thermal-energy conditions can open at higher collisional energies. In addition, one can compare conditions in which the molecular system has, using equipartition of energy, $1/2kT$ (or 0.026 eV at $T=300$ K) available to it in each degree of freedom (translational, vibrational, and rotational), to one in which the molecular intermediate state has enormous energy (5 eV say, or 58 000 K) in just one (here, the translational) degree of freedom. For example, in a study of the reaction [1] $HF+Ba \rightarrow BaF+H$ it was shown that as the center-of-mass (c.m.) translational energy was varied between 0.056 and 0.56 eV, the excess energy appeared mainly as product translational energy, with smaller amounts in rotational and vibrational excitation of BaF. Similarly, in a study of the reaction of fast H atoms with N_2O [2] a channel which is endoergic by 1.4 eV [$H+N_2O \rightarrow NH+NO$] was found to occur with equal probability to one exoergic by 2.73 eV [$H+N_2O \rightarrow OH+N_2$]. The translational energy of H in this study [2] was bimodal at 2.7 eV (85%) and 2.2 eV (15%).

At thermal energies, and at temperatures (in the Maxwell-Boltzmann equilibrium sense) as high as 1000 K (or $3/2kT=0.13$ eV for the three translational degrees of freedom), the reaction of $O(^3P)$ with HCN proceeds through the channels:

$$O(^3P)+HCN(\tilde{X})-0.07\ \text{eV} \rightarrow NCO(\tilde{X})+H(1S)\ , \quad (1)$$

$$O(^3P)+HCN(\tilde{X})+1.43\ \text{eV} \rightarrow CO(X)+NH(X)\ , \quad (2)$$

$$O(^3P)+HCN(\tilde{X})+0.93\ \text{eV} \rightarrow OH(X)+CN(X)\ . \quad (3)$$

The rate coefficients for these reactions have been reviewed [3], and the overall rate coefficient [sum of reactions (1)–(3)] is reasonably well established: $8.6\times10^{-12}e^{(-4090/T)}$ [units of $cm^3/(molecule\ s)$] in the temperature range $T=450$–650 K and $1.94\times10^{-10}e^{(-7460/T)}$ in the range 1800–2500 K. The individual rate coefficients have large uncertainties and are approximately given by [3]

$$k_1=1.2\times10^{-10}e^{(-7460/T)},$$

$$k_2=3.7\times10^{-11}e^{(-7740/T)},$$

and

$$k_3<8.3\times10^{-11}e^{(-11000/T)}\ .$$

The ergicities are estimated to be −11.5 kJ/mol (−0.12 eV), −119 kJ/mol (−1.23 eV), and +89.9 kJ/mol (0.93 eV) for reactions (1), (2), and (3), respectively [3]. Under energy-equipartition conditions one would thus expect reaction (1) to proceed rapidly, with slower rates for reactions (2) and (3).

Reported herein is a study of the reaction of fast [laboratory (lab) energies of 5–25 eV] $O(^3P)$ atoms with HCN under single-collision conditions. The study was undertaken to identify the channel(s) which are active in the hyperthermal energy regime. One may also investigate the effect of increasing collision energy on internal electron excitation of the products. For example, the formation of excited electronic states in reactions (2) and (3) requires that extra energy be provided to the reactants (electronic energies are from Ref. [4]):

$$O(^3P)+HCN(\tilde{X})+2.3\ eV\rightarrow CO(X\,^1\Sigma^+)+NH(A\,^3\Pi_i)\ , \tag{2'}$$

$$O(^3P)+HCN(\tilde{X})+4.1\ eV\rightarrow OH(X\,^2\Pi_i)+CN(B\,^2\Sigma^+)\ . \tag{3'}$$

In addition to this intrinsic interest in high kinetic-energy reactions the advent of space exploration and space-borne observing platforms has revealed new phenomena. Studies of spacecraft surfaces and the surrounding atmosphere in a low earth orbit have indicated that the CN $B\rightarrow X$ emission is observed when the spacecraft shuttle-engine-exhaust species (including HCN as partially combusted fuel) collide with the atmosphere [5]. A spacecraft in a low earth orbit travels at approximately 7.8 km/s (depending on its altitude, with relevant altitudes in the range 300–1000 km). The spacecraft surface and the surrounding gaseous envelope collide at this velocity with the atmosphere, which consists of approximately 70% $O(^3P)$ atoms at 300-km altitude. Surfaces facing the direction of travel have been observed to glow in the visible spectral region (for a review, see Ref. [6]). The emission is continuous at a spectral resolution of 3.4 nm [7,8] and has been attributed to electronically excited NO_2 [7]. In this example, incoming fast O atoms recombine with NO, and the translational energy is converted into electronic excitation of the NO_2, and into a high translational energy of the emitting NO_2^* as it departs the spacecraft surface [7,9].

II. EXPERIMENTAL METHODS

The atomic-oxygen source, target region, and spectrometer system used in these measurements were the same as those used previously in single-collision, beam-beam collision studies of the gaseous targets H_2O, CO_2 [10], and N_2H_4 [11]. By way of summary, the collision measurements are carried out in uniform, high-intensity (6 T) solenoidal magnetic field (see Fig. 1 of Ref. [12]). Magnetically confined electrons of 8.0-eV energy attach to a beam of NO to form $N+O^-(^2P)$. The magnetically confined O^- ions are accelerated to the desired final energy and are separated from the electrons by a trochoidal deflector. The electrons are photodetached from the O^- ions using all visible lines from a 20-W argon-ion laser in a multiple-pass geometry. The detachment fraction is 8–15%, depending upon the velocity of the O^- ions through the detachment region (see below). The resulting O atoms are left exclusively in the ground ^3P state. The O and (undetached) O^- beams are then directed towards the HCN target. The O^- ions, and any photodetached electrons, are reflected prior to reaching the HCN beam by a negative bias on the emission-collection mirror before the target. The neutral HCN beam itself is formed by effusion through a 1.0-mm-diam hypodermic nozzle. The target region was differentially pumped with a cryopump to maintain a pressure difference of 1.3×10^{-4} Pa (source) and 2.7×10^{-6} Pa (target) during operation. Base pressures were 1×10^{-6} and 7×10^{-8} Pa at the source and target, respectively.

Optical emissions from the collision region are collected with a spherical mirror and focused onto the entrance plane of a double-grating monochromator. Separate spectra of the emissions and backgrounds are recorded via multichannel scaling. The spectral resolution is 4.0 nm [full width at half maximum (FWHM)]. The principal sources of backgrounds are O^- collisions with surfaces and, in the wavelength range 450–550 nm, scattered light from the argon-ion laser and the directly heated electron emitter. The HCN was obtained commercially [13] and had a stated purity of greater than 99.5% with the remaining impurities being H_2O (<0.5%) and H_2SO_4 stabilizer (0.1%). The purity was verified by measuring the fractionation pattern of the HCN with a quadrupole mass analyzer. A base peak of 27 amu was found, with no trace at the 0.5–1% level of other impurities, especially C_2N_2 at 52 amu [14]. The HCN was contained in a stainless-steel cylinder, and was subjected to ten freeze-thaw cycles with liquid nitrogen to remove dissolved gases. All valves and transfer lines were stainless steel.

III. RESULTS AND DISCUSSION

A. Emission spectra

The relation between laboratory and c.m. energies is given by the standard expression [16]

$$E_{\text{c.m.}}=\frac{m_1m_2}{m_1+m_2}\left\{\frac{E_1}{m_1}+\frac{E_2}{m_2}-2\left[\frac{E_1E_2}{m_1m_2}\right]^{1/2}\cos\theta\right\}\ , \tag{4}$$

where m_i and E_i are masses and laboratory energies (subscripts 1 and 2 refer to O and HCN, respectively). The energy of the HCN molecules in the beam is thermal ($E_2=0.04$ eV), and the angle θ between the O and HCN beams is 90° for crossed-beam collisions. Contribution from the second term in Eq. (4) (order of 0.01 eV c.m. energy) is neglected, as is the effect (third term, order of 0.01 eV c.m. energy) of the HCN beam angular width. In this case Eq. (4) reduces to $E_{\text{c.m.}}=0.628E_1$. Equation (4) is based only upon the laboratory energies of the incident particles and gives no information on the energy sharing between the outgoing particles in the given reaction channel.

Shown in Fig. 1 are spectra of the CN $A\rightarrow X$ and $B\rightarrow X$ emission systems resulting from the collisions of O and HCN. Also shown is a simulation of the $A\rightarrow X$ emission in terms of energy locations [4] and Franck-Condon factors [15] of the vibrational bands. The laboratory energy for the O+HCN collision system was 20.0 eV, corresponding to a c.m. energy of 12.6 eV. The $B\rightarrow X$ band system in Fig. 1 is approximately two orders of magnitude more intense than the $A\rightarrow X$ system. It is shown in more detail in Fig. 2 at a lab energy of 10.6 eV (6.7 eV c.m.). Here one has contributions from three main sequences: $\Delta v=+1$ centered at 358 nm, $\Delta v=0$ at 387 nm, and $\Delta v=-1$ at 417 nm. In addition, a nonlocal-thermodynamic-equilibrium computer code was used to characterize the emitting B state in terms of a

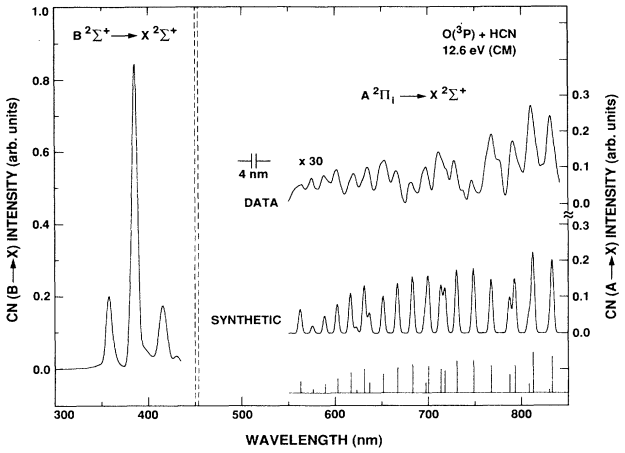

FIG. 1. Measured and simulated spectra of the CN $A \rightarrow X$ emission system in the wavelength range 550–850 nm, at a lab energy of 20 eV (12.6-eV c.m. energy). Also shown is the CN $B \rightarrow X$ emission in the range 300–440 nm (see Fig. 2).

separate vibrational T_v and rotational T_r temperature [17]. All important vibrational bands up to $v'=v''=9$ were included, as well as all rotational states in each v', v'' level whose rotational energy did not exceed 2×10^4 cm^{-1} (2.5 eV). Oscillator strengths were taken from Ref. [15]. A Boltzmann distribution of population in the B state was used. Results are shown (solid line) for the combination $T_v=7000$ K (0.60 eV) and $T_r=2000$ K (0.17 eV). The agreement between experiment and simulation is within the combined uncertainties.

B. Reaction threshold

Central to specifying the appropriate reaction channel is the threshold energy of the channel. This measurement in turn relies on accurate knowledge of the energy distribution of the O(^3P) atoms in the beam. This energy distribution was obtained from the energy distribution of the $O^-(^3P)$ ions: the approximately 1.0-eV excess c.m. energy in the photon absorption-detachment process is shared between the outgoing O(^3P) atom and the electron, with the lighter electron taking up practically all the excess energy. And hence the energy distribution of the detached O(^3P) atom (after correction for the changing detachment efficiency with velocity, see below) will be very nearly identical to that of the $O^-(^2P)$ ion, to within the ratio m_1/m_e (electron mass m_e).

The magnetic confinement of the O^- ions made for a convenient retarding-potential difference (RPD) geometry. The retardation and ion detection was carried out by means of a biasing grid placed before the sample holder used as a Faraday cup. Measurements were made of O^- current as a function of negative retarding voltage on the grid. Results of the retarded current are shown in Fig. 3.

The RPD technique measures the axial width of the particles in the beam. One may also estimate the broadening in the radial direction due to the O^- space charge. Balance between the repulsive force $\mathbf{F}_r=e\mathbf{E}_r$ of the radial electric field $\mathbf{E}_r$ and the centripetal force $\mathbf{F}_c=e\mathbf{v}_\theta\times\mathbf{B}$ of the confined, spiraling ions ($\mathbf{v}_\theta$ is the ion tangential velocity) provides a measure of the rotational kinetic energy $T_\theta=1/2mv_\theta^2$. Under the present experimental conditions of beam diameter, energy and current T_θ was calculated to be less than 0.1 eV. This was also verified by observing the diameter of an eroded spot on a silver thin film placed in the O(^3P) beam. One obtains a divergence half-angle from the diameter, and hence T_θ. The value obtained in this measurement was 0.06 eV at 8-eV (lab) O(^3P) energy, so that effects of the radial ener-

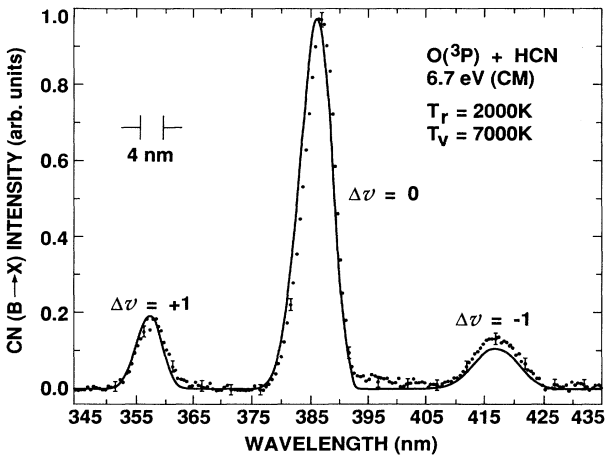

FIG. 2. Measured (●) and simulated (——) spectra of the CN ($B \rightarrow X$) emission system at 6.7-eV c.m. energy. The $\Delta v=v'-v''=0$, +1, and −1 sequences are shown. The simulated spectrum corresponds to vibrational and rotational temperatures of $T_v=7000$ K (0.60 eV) and $T_r=2000$ K (0.17 eV), respectively [17].

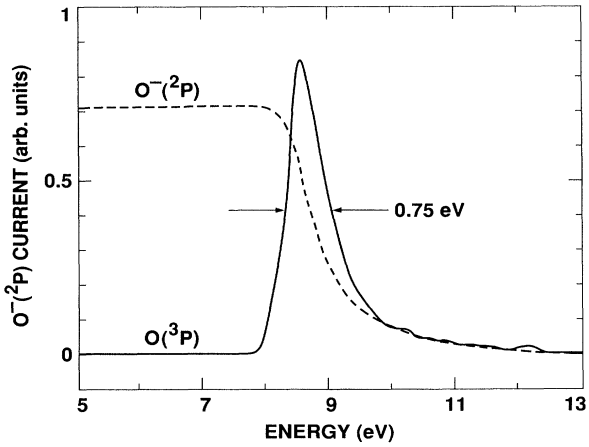

FIG. 3. Energy distribution of the $O^-(^2P)$ ions at an ion current of 0.71 μa, as obtained by retarding-potential difference (RPD) measurements. Shown are the O^- RPD curve and the O(^3P) distribution obtained from the derivative of the O^- RPD curve, corrected for the variation of detachment efficiency with energy. The peak energy is 8.6±0.2 eV, and the FWHM is 0.75±0.01 eV.

gy width were considered negligible.

In order to convert the derivative of the $O^-(^2P)$ RPD curve to an $O(^3P)$ distribution one must correct for the changing O^- detachment efficiency with particle velocity through the multiple-pass detachment mirrors. This changing efficiency will distort the derivative, since the lower-energy portion of the O^- distribution will be more efficiently detached than the higher-energy portion. The detachment efficiency g was determined experimentally and can be expressed in terms of known experimental parameters

$$g(V)=1-\exp(-f\sigma L/V)\ , \tag{5}$$

where f is the laser flux [photons/(cm^2 s)], σ the detachment cross section (cm^2), L the total path length in the multiple-pass mirrors (cm), and V the O^- velocity (cm/s). The variation of g with V was obtained by measurement of the change in O^- current in the biased-grid Faraday cup near the beam target, as a function of the O^- energy. (When the laser is turned on, the O^- current decreases due to photodetachment.) The correction factor was then applied to the derivative of the experimentally observed RPD curve [$O^-(^2P)$ curve in Fig. 3)] and the $O(^3P)$ energy distribution was obtained. The width of the $O(^3P)$ distribution (Fig. 3) at the indicated O^- current (0.71 μa) was 0.73 eV (FWHM). The lab energy of $O(^3P)$ in Fig. 3 was 8.6 eV. The $O^-(^2P)$ RPD curves were measured at ten energies in the range 5–25 eV and were found to be unchanged, within experimental error. The $O(^3P)$ distributions were then calculated at each energy through Eq. (5).

The $O(^3P)$ energy is known to within the difference in contact potentials of the metals (W and Ti) used in the system. This difference, and hence the maximum uncertainty in the O-atom energy, is estimated to be ± 0.2 eV [18].

With the monochromator detection wavelength fixed at 387 nm (peak of the $\Delta v=0$ sequence in the $B\rightarrow X$ emission), the emission intensity was monitored as a function of $O(^3P)$ energy. Results of this measurement are shown in Fig. 4. By unfolding the $O(^3P)$ energy distribution (Fig. 3) from the data one obtains an energy threshold of 7.4 ± 0.8 eV (lab), or 4.6 ± 0.5 eV (c.m.), with the principal source of uncertainty due to poor counting statistics at the threshold. The threshold energy is very likely an upper limit since (a) it includes additional rotational, vibrational, and translational energy in the OH and CN products, and (b) thresholds generally trend to lower values with any increase in the instrumental signal-to-background ratio. It is possible with this measurement to determine that the reaction channel is reaction (3′). From the enthalpies of reaction, the energy required for reaction and excitation to the B level at 387 nm is 5.25 (H—CN bond energy) -4.35 (O—H bond energy) $+3.20$ (B-state energy) $=4.10$ eV (c.m.) or 6.53 eV (lab). This is in good agreement with measurement (4.6 ± 0.5-eV c.m.), especially with the caveats above.

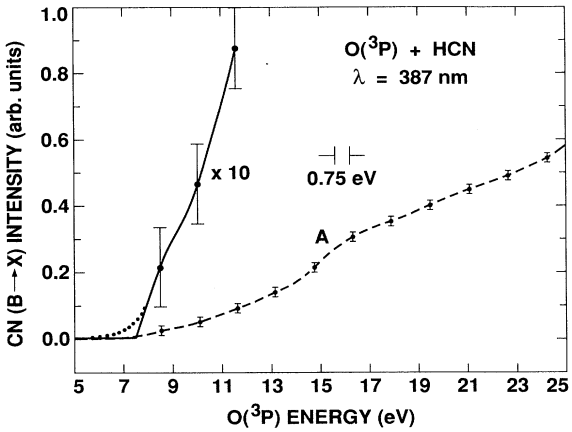

FIG. 4. Excitation of the $B\rightarrow X$ emission at 387 nm as a function of $O(^3P)$ lab energy in the range 5–25 eV (curve A). The excitation function has been deconvoluted from the energy distribution of the $O(^3P)$ atoms (see Fig. 3), and the excitation threshold is measured to be 7.4 ± 0.8 eV (lab, from curve $A\times10$). Dotted portion at threshold (· · · ·) is the intensity without deconvolution, showing effects of the high-energy tail in Fig. 3.

C. Reaction dynamics

Reaction (2′), even though requiring less energy than reaction (3′), is not detected. The NH $A\rightarrow X$ transition is strong, peaks at 337.5 nm [11], and is absent from the spectra. HCN in its ground state is linear, with configuration H—C—N. Reaction (2′) requires a molecular rearrangement, perhaps to the H—N—C configuration. This configuration is known to lie 0.625 ± 0.04 eV above the H—C—N configuration [19]. Moreover, *ab initio* calculations predict a barrier to the conversion, with the transition state lying 1.94 ± 0.04 eV above the H—C—N energy [20]. Hence an energy of about 4.2 eV is required for reaction (2′) to occur. By contrast, reaction (3′) requires less energy and can proceed by a simpler ("harpoon") mechanism wherein the H atom can be stripped from the CN portion by the incident O atom [21]. It is interesting to speculate on the conditions which might allow reaction (2′) to occur. One possible scenario is to pump the energy required to reach the transition state into HCN vibrational modes. Collisions with $O(^3P)$ could then lead to the formation of NH(A).

ACKNOWLEDGMENTS

We thank L. Bernstein for his simulated spectra of the $B\rightarrow X$ emission system. This work was carried out at the Jet Propulsion Laboratory, California Institute of Technology, and was supported by the AFOSR, Phillips Laboratory, and SDIO/TNS through agreement with the National Aeronautics and Space Administration.

[1] A. Gupta, D. S. Perry, and R. N. Zare, J. Chem. Phys. **72**, 6237 (1980).
[2] G. Hoffmann, D. Oh, H. Iams, and C. Wittig, Chem. Phys. Lett. **155**, 356 (1989).
[3] D. L. Baulch, C. J. Cobos, R. A. Cox, C. Esser, P. Frank, Th. Just, J. A. Kerr, M. J. Pilling, J. Troe, R. W. Walker, and J. Warnatz, J. Phys. Chem. Ref. Data **21**, 411 (1992).
[4] K. P. Huber and G. Herzberg, *Molecular Spectra and Molecular Structure IV. Constants of Diatomic Molecules* (Van Nostrand Reinhold, New York, 1979), p. 154.
[5] R. A. Viereck, L. S. Bernstein, S. B. Mende, E. Murad, G. R. Swenson, and C. B. Pike, J. Spacecr. Rockets (to be published).
[6] H. B. Garrett, A. Chutjian, and S. Gabriel, J. Spacecr. Rockets **25**, 321 (1988).
[7] G. R. Swenson, S. B. Mende, and K. S. Clifton, Geophys. Res. Lett. **12**, 97 (1985).
[8] R. A. Viereck, S. B. Mende, E. Murad, G. R. Swenson, C. P. Pike, F. L. Culbertson, and R. C. Springer, Geophys. Res. Lett. **19**, 1219 (1992).
[9] R. A. Viereck, E. Murad, B. D. Green, P. Joshi, C. P. Pike, R. Hieb, and G. Harbaugh, Nature **354**, 48 (1991).
[10] O. J. Orient, A. Chutjian, and E. Murad, Phys. Rev. Lett. **65**, 2359 (1990).
[11] O. J. Orient, K. E. Martus, A. Chutjian, and E. Murad, J. Chem. Phys. **97**, 4111 (1992).
[12] O. J. Orient, K. E. Martus, A. Chutjian, and E. Murad, Phys. Rev. A **45**, 2998 (1992).
[13] FUMICO, Inc., Amarillo, TX.
[14] *EPA/NIH Mass Spectral Data Base,* Natl. Stand. Ref. Data Syst., Natl. Bur. Stand., edited by S. R. Heller and G. W. A. Milne (U.S. GPO, Washington, DC, 1978), Vol. 1.
[15] H. Lavendy, G. Gandara, and J. M. Robbe, J. Mol. Spectrosc. **106**, 395 (1984).
[16] K. T. Dolder and B. Peart, Rep. Prog. Phys. **39**, 693 (1976).
[17] A. Berk, L. S. Bernstein, S. C. Richtsmeier, J. W. Cox, and M. W. Slack (private communication).
[18] *Handbook of Chemistry and Physics,* 70th ed. (CRC, Boca Raton, FL, 1989), pp. E-93 and 94.
[19] C.-F. Pau and W. J. Hehre, J. Phys. Chem. **86**, 321 (1982).
[20] T. J. Lee and A. P. Rendell, Chem. Phys. Lett. **177**, 491 (1991).
[21] I. W. M. Smith, *Kinetics and Dynamics of Elementary Gas Reactions* (Butterworth, Boston, 1980).